

Resistive drift wave test of the 2DX code

D. A. Baver and J. R. Myra

Lodestar Research Corporation, Boulder Colorado 80301

Maxim Umansky

Lawrence Livermore National Laboratory

1 Introduction

This test was devised to verify the ability of the 2DX eigenvalue code to correctly solve a simple fluid model relevant to edge turbulence in tokamaks. Since the functionality of the 2DX code depends on both the source code itself and the input file defining the system of equations to solve (structure file), this test demonstrates both. Since a similar test was performed on an earlier version of 2DX, this verifies that the current version retains this functionality. Moreover, since the structure file for this test represents a subset of a more general 6-field model, many of the terms in that test are also verified.

This test compares 2DX results to an exact analytic solution for the model equations of interest.

2 Description

2.1 Code structure

The 2DX code is a highly flexible eigenvalue solver designed for problems relevant to edge physics in toroidal plasma devices. Its flexibility stems from the use of a specialized input file containing instructions on how to set up a particular set of equations. Because of this, the 2DX code permits model equations to be changed without altering its source code. The drawback to this approach is that any change to the structure file represents a potential source of error, necessitating re-verification. This problem is offset by the fact that the source code remains unchanged, thus testing one structure file builds confidence in the underlying code that interprets the structure file. Also, structure files can be translated into analytic form, thus allowing the user to verify that the file contains the equations intended.

The structure file contains two main parts: an elements section, which constructs the differential operators and other functions used in a particular set

of equations, and a formula section, which assembles these into an actual set of equations. This separation means that elements can be recycled in other structure files. By testing one structure file, one builds confidence in the elements used in that file. The main source of error when switching to a different structure file then is in the formula section, which can be manually verified by translating into analytic form.

Regardless of the content of the structure file, the 2DX code is fundamentally a finite-difference eigenvalue solver. As such, it is subject to the limitations of any code of its type.

2.2 Model equations

For the resistive drift wave test, two different model equations are used [1]-[2]. One of these models is electrostatic, the other includes electromagnetic effects.

The electrostatic case uses the following equations:

$$\gamma \nabla_{\perp}^2 \delta \Phi = -\frac{B^2}{n} \partial_{\parallel} \nabla_{\perp}^2 \delta A \quad (1)$$

$$\gamma \delta n = -\delta v_E \cdot \nabla n \quad (2)$$

$$-\gamma \nabla_{\perp}^2 \delta A = \nu_e \nabla_{\perp}^2 \delta A - \mu n \nabla_{\parallel} \delta \Phi + \mu T_e \nabla_{\parallel} \delta n \quad (3)$$

where

$$\delta p = (T_e + T_i) \delta n + n(\delta T_e + \delta T_i) \quad (4)$$

$$C_r = \mathbf{b} \times \kappa \cdot \nabla = -\kappa_g R B_p \partial_x + i(\kappa_n k_b - \kappa_g k_{\psi}) \quad (5)$$

$$\nabla_{\perp}^2 = -k_b^2 - jB(k_{\psi} - i\partial_x R B_p)(1/jB)(k_{\psi} - iR B_p \partial_x) \quad (6)$$

$$\partial_{\parallel} Q = B \nabla_{\parallel} (Q/B) \quad (7)$$

$$\nabla_{\parallel} = j \partial_y \quad (8)$$

$$\delta v_E \cdot \nabla Q = -i \frac{k_z (R B_p \partial_x Q)}{B} \delta \Phi \quad (9)$$

$$\nu_e = .51 \nu_r n / T_e^{3/2} \quad (10)$$

The electromagnetic model uses the following alternate equation set:

$$\gamma \nabla_{\perp}^2 \delta \Phi = -\frac{B^2}{n} \partial_{\parallel} \nabla_{\perp}^2 \delta A \quad (11)$$

$$\gamma \delta n = -\delta v_E \cdot \nabla n \quad (12)$$

$$\gamma \left(\frac{n}{\delta_{er}^2} - \nabla_{\perp}^2 \delta A \right) = \nu_e \nabla_{\perp}^2 \delta A - \mu n \nabla_{\parallel} \delta \Phi + \mu T_e \nabla_{\parallel} \delta n + \mu T_e \delta \mathbf{b} \times \nabla n \quad (13)$$

where δ_{er} is the Bohm-normalized value of skin depth for the reference parameters and:

$$\delta \mathbf{b} \times \nabla Q = \frac{ik_b(\partial_r Q)}{\mu\delta_{er}^2 b} \delta A \quad (14)$$

2.3 Boundary conditions

This test case uses phase-shift periodic boundary conditions in the parallel direction, and zero-derivative boundary conditions in the radial direction. The phase shift in the parallel direction is given by:

$$e^{i2\pi nq} \quad (15)$$

For this particular case, q is set to an integer so as to establish a simple periodic domain.

2.4 Profile setup

The formulas in Eq. 1-13 are normalized to Bohm units. Values are converted by dividing input distances by ρ_s , and input magnetic fields are in Tesla. Output eigenvalues are multiplied by ω_{ci} . Resistivity is given by the formula:

$$\nu_r = \frac{\mu_u}{.51\sigma} \quad (16)$$

where

$$\sigma = 1.96 \frac{\omega_{ce}}{\nu_{ei}} \quad (17)$$

The geometry used is a periodic slab. Curvature effects are included in the equation set, but curvature is set to zero. Zero-derivative boundary conditions are used in the radial direction, and the domain is set to only two grid cells wide in that direction. This is done so as to approximate a 1-D problem using a 2-D code, and because the 2DX code cannot simulate domains that are only one grid cell wide in either direction.

The Jacobian factor used to calculate parallel derivatives is set so as to fix the parallel wavenumber of the fundamental mode of the system. As we will see later, the fundamental mode may or may not be the fastest growing mode depending on what wavenumber is selected. Setting the wavenumber of the fundamental mode is accomplished by simply having parallel positions range from π to $-\pi$ and setting the Jacobian equal to k_{\parallel} .

3 Analytic results

Since both the electrostatic and electromagnetic resistive drift wave models are tested in homogenous domains, they can be solved analytically by taking a Fourier transform in both directions. This allows the systems of differential equations to be reduced to algebraic matrix equations. Assuming that $\nabla_{\perp}^2 = -k_b^2$, this yields an eigenvalue problem of the form $Ax = \gamma x$, where A for the electrostatic model is:

$$\begin{bmatrix} 0 & -ik_b RB_p n / BL_n & 0 \\ 0 & 0 & -iBk_{\parallel} / n \\ ik_{\parallel} T / \beta_r \delta_{er}^2 k_b^2 & -ik_{\parallel} n / \beta_r \delta_{er}^2 k_b^2 & -.51\nu_r n / T^{3/2} \end{bmatrix} \quad (18)$$

and for the electromagnetic model:

$$\begin{bmatrix} 0 & -ik_b RB_p n / BL_n & 0 \\ 0 & 0 & -iBk_{\parallel} / n \\ \frac{ik_{\parallel} T / \beta_r n}{1 + \delta_{er}^2 k_b^2 / n} & \frac{-ik_{\parallel} 1 / \beta_r}{1 + \delta_{er}^2 k_b^2 / n} & \frac{-iTk_b RB_p / BL_n - .51\delta_{er}^2 \nu_r k_b^2 / T^{3/2}}{1 + \delta_{er}^2 k_b^2 / n} \end{bmatrix} \quad (19)$$

These can be solved using standard eigenvalue solving routines. The results of this calculation are shown in Figs. 1-2 along with the numerical results from 2DX.

4 Numerical results

The code was tested by sweeping the dimensionless variable σ_{\parallel} from .1 to 100 and plotting the fastest growing eigenvalue. In addition, the fastest growing value at the fundamental wavenumber was also calculated. The parameters used in this test are as follows:

$$\begin{aligned} \delta_{er}^2 &= 4 \\ \beta_r &= .02 \\ \nu_r &= .05 \\ RB_p &= 1 \\ k_b &= 1/\delta_{er} \\ n &= 1 \\ n' &= -1/L_n \\ B &= 1 \\ T_e &= 1 \\ L_n &= (RB_p n T_e^{3/2} / B) / (.51\nu_r / \delta_{er}) \\ k_{\parallel} &= \omega_s \sqrt{\beta_r \sigma_{\parallel}} \\ \omega_s &= k_b RB_p n / BL_n \end{aligned}$$

The input data for these test cases is also shown in table 1.

The results of this are shown in Fig. 1-2. The data for these plots is additionally shown in tables 2-3. In these figures, the upper curves are growth rates while the lower curves are frequencies. The lines are analytic solutions, and the dots are numerical solutions.

The two sets of dots arise because the analytic solution assumes that the parallel wavenumber is equal to the smallest nonzero wavenumber possible for a given size domain. This is not true for large domain sizes, since in that case the fastest growing mode has a wavelength shorter than the domain size. For this reason, if the eigenvalue solver returns the fastest growing mode it will not agree with the analytic solution for low σ_{\parallel} . The solution to this is to return a number of fast-growing eigenmodes and sort them by parallel wavenumber, which can be calculated from the eigenvector. This returns the growth rate of the fundamental (longest wavelength) mode, which agrees with the analytic solution.

References

- [1] W. Horton, Rev. Mod. Phys. **71**, 735 (1999).
- [2] M. Wakatani and A. Hasegawa, Phys. Fluids **27**, 611 (1984).

nx	2	ny	64
dx	100000	dy	.0997331
ω_{ci}	39.2156862745098	n	0
μ	12.5	ν_r	0.05
q	0	k_b	.5
j	$.00360624\sqrt{\sigma_{\parallel}}$	k_{ψ}	0
κ_n	0	κ_g	0
B	1	RB_p	1
n_0	1	T_e	1
n'_0	-.051	δ_{er}^2	4

Table 1: Non-dimensional profile functions and parameters used in the resistive drift wave test case, as a function of the parameter σ_{\parallel} .

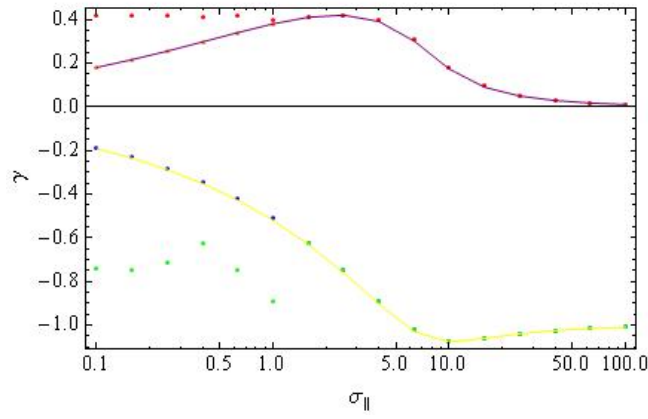


Figure 1: Growth rate vs. parallel scale for electrostatic RDW model. Upper curves are growth rates, lower curves are frequencies. Yellow/purple curves are analytic solutions, orange/blue points are 2DX results for the fundamental mode, red/green points are 2DX results for the dominant mode.

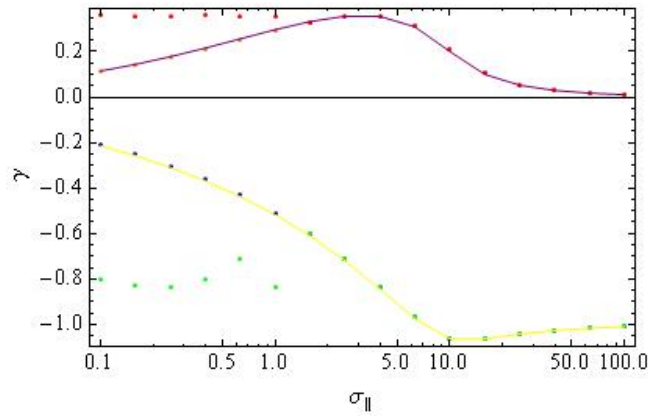


Figure 2: Growth rate vs. parallel scale for electromagnetic RDW model. Upper curves are growth rates, lower curves are frequencies. Yellow/purple curves are analytic solutions, orange/blue points are 2DX results for the fundamental mode, red/green points are 2DX results for the dominant mode.

$\sigma_{\parallel}/\sigma_{\perp}$	γ (fundamental)	γ (dominant)	γ (analytic)
.1	.178224	.420647	.180541
.158489	.213252	.420558	.215866
.251189	.252259	.420242	.255123
.398107	.294227	.408777	.297238
.630957	.337129	.420527	.340093
1	.377343	.395195	.379923
1.58489	.408656	.408656	.410281
2.51189	.420541	.420542	.420245
3.98107	.395456	.395457	.391685
6.30957	.310130	.310130	.301662
10	.181312	.181313	.173175
15.8489	.093838	.0938385	.0897538
25.1189	.051386	.0513868	.0493784
39.8107	.029746	.0297466	.0286701
63.0957	.017815	.0178157	.0172016
100	.010887	.0108879	.0105238

Table 2: Growth rate vs. parallel scale for electrostatic RDW model.

$\sigma_{\parallel}/\sigma_{\perp}$	γ (fundamental)	γ (dominant)	γ (analytic)
.1	.113059	.359233	.114909
.158489	.14177	.357119	.143972
.251189	.175374	.35643	.1779
.398107	.213144	.359023	.215916
.630957	.253536	.35487	.256408
1	.293914	.35626	.296647
1.58489	.330003	.330003	.332215
2.51189	.35479	.35479	.355837
3.98107	.356342	.356342	.355114
6.30957	.314289	.314289	.309006
10	.209467	.209467	.200683
15.8489	.105075	.105075	.100045
25.1189	.0545967	.0545967	.052327
39.8107	.0307527	.0307527	.029601
63.0957	.0181601	.0181601	.0175218
100	.0110127	.0110127	.0106402

Table 3: Growth rate vs. parallel scale for electromagnetic RDW model.